J Mol Model (2012) 18:4893–4900
DOI 10.1007/s00894-012-1488-y

ORIGINAL PAPER

Quantum chemical study in the direction to design efficient donor-bridge-acceptor triphenylamine sensitizers with improved electron injection

Ahmad Irfan · Abdullah G. Al-Sehemi

Received: 14 April 2012 / Accepted: 28 May 2012 / Published online: 21 June 2012

Abstract The ground state geometries have been computed by using density functional theory. The excitation energies for dye sensitizers were performed by using time dependant density functional theory. The polarizable continuum model (PCM) has been used for evaluating bulk solvent effects at all stages. The calculations have been carried out in methanol according to the experimental set up. The long-range-corrected functional (PCM-TD-LC-BLYP) underestimate the absorption spectrum of parent molecule while PCM-TDBHandHLYP is in good agreement with the experimental data. The highest occupied molecular orbital (HOMO) is delocalized on TPA moiety while lowest unoccupied molecular orbital (LUMO) is localized on anchoring group, conjugated chain and the benzene ring near to the anchoring group. The LUMO energies of all the investigated dyes are above the conduction band of TiO_2, HOMOs are below the redox couple and HOMO-LUMO energy gaps of studied dyes are smaller compared to TC4. The **1** and **3** are 7 and 12 nm blue shifted while **2** and **4** are 25 and 22 nm red shifted, respectively compared to TC4. The trend of electron injection (ΔG^{inject}), relative electron injection (ΔG_r^{inject}), and electronic coupling constant (|VRP|) has been observed as **3**>**1**>**4**>**2**>TC4. The improved ΔG^{inject}, |VRP| and light harvesting efficiency (LHE) of new designed sensitizers revealed that these materials would be excellent sensitizers. The broken coplanarity between the benzene near anchoring group having LUMO and the last benzene attached to TPA unit in **1**–**4** consequently would hamper the recombination reaction.

Keywords Absorption · Dye-sensitized solar cells · Electron injection · Highest occupied molecular orbitals · Lowest unoccupied molecular orbitals

Introduction

Dye-sensitized solar cells (DSCs) are currently attracting considerable attention because of their high light-to-electricity conversion efficiencies, ease of fabrication, and low production costs [1–3]. The sensitizer is a crucial element in DSCs, exerting significant influence on the power conversion efficiency as well as the stability of the devices. The Ruthenium complexes photosensitizers show a solar energy-to electricity conversion efficiency of 10 % in average [2]. Metal free organic DSCs have advantages over metal containing sensitizers, e.g., simple and inexpensive preparation processes, environment friendly and high molar extinction coefficient [4]. Different metal free dyes have been investigated which have shown comparable efficiencies to metal containing sensitizers [5–9]. Until now, it remains a severe challenge for both experiment and theory to elucidate the fundamental properties of the ultrafast electron injection [10], and to approach the satisfied efficiency of DSCs. Further developments to design dye will play a crucial part in the ongoing optimization of DSCs [11], and it depends on the quantitative knowledge of dye sensitizer.

Electronic supplementary material The online version of this article (doi:10.1007/s00894-012-1488-y) contains supplementary material, which is available to authorized users.

A. Irfan (✉) · A. G. Al-Sehemi
Chemistry Department, Faculty of Science,
King Khalid University,
Abha, Saudi Arabia
e-mail: irfaahmad@gmail.com

To improve the efficiency of the UV/vis photoinduced intramolecular charge transfer most of the organic sensitizers are made of a donor, a bridge and acceptor (DBA) moieties. The good conjugation across the donor and anchoring group determines the large charge transfer character of the electronic transition. The dye aggregation and charge recombination can lead to lower efficiency in organic sensitizers [12–14]. It has been found that triphenylamine (TPA) [15] derivatives as electron donor and the cyanoacetic acid moiety as electron acceptor are good choices to improve the efficiency [12, 16]. It is expected that TPA can restrain the cationic charge from the semiconductor surface therefore hinder the recombination. TPA also features a steric hindrance that can prevent unfavorable dye aggregation at the semiconductor surface [16]. To model and design efficient metal-free sensitizers for DSCs, appropriate DBA systems are required whose properties can be tuned by applying the passable structural modifications. To enhance the electron donor ability of TPA moiety Xu et al. synthesized the TC4 where vinyl unit has been substituted at position **3** [17]. The efficiency has been observed 4.82 % for 2-cyano-5-(4-(phenyl(4-vinylphenyl)amino)phenyl) penta-2,4-dienoic acid (TC4) [17]. Recently, we showed that substitution of vinyl at position **3** and **3'** are more favorable toward enhancing the electron injection and reducing the HOMO-LUMO energy gap [18]. It is well known that CH_3 enhance the electron donor ability [19]. The sensitizers that where charge transferred from donor to acceptor moiety are good toward high efficiency [20–22]. In our previous study we pointed out that by replacing two hydrogens with donor group can lead to higher efficiency, thus to augment the donor ability of TPA unit we have replaced the two hydrogens of vinyl by CH_3. Moreover, to check the effect of bridge on the electronic properties we have extended the benzene rings; two benzene rings between TPA moiety and anchoring group (**1** and **2**), three benzene rings (**3** and **4**). In TC4 there are two double bonds between TPA moiety and anchoring group as bridge. In our new designed sensitizers, we have extended this bridge as well by increasing the double bonds up to three (**1** and **3**) and four (**2** and **4**) to enhance the conjugation pathway between last benzene and anchoring group, see Fig. 1. It has been esteemed that by improving the donor ability and elongating the bridge, efficient sensitizers would be modeled.

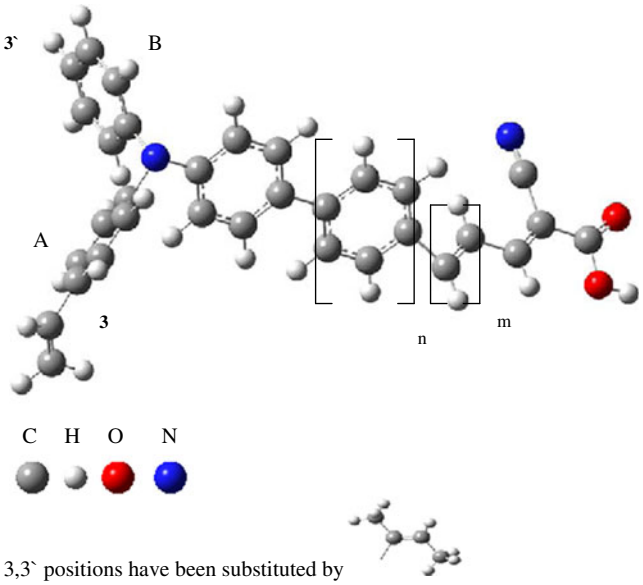

3,3` positions have been substituted by TC4, n=0, m=1
1, n=2, m=2
2, n=2, m=3
3, n=3, m=2
4, n=3, m=3

Fig. 1 The structures of **1**–**4** investigated in present study

Computational details

The computations of the geometries, electronic structures, as well as electronic absorption spectra for dye sensitizers were performed using density functional theory (DFT) and time dependant density functional theory (TD-DFT) with Gaussian09 package [23]. The DFT was treated according to Becke's three parameter gradient-corrected exchange potential and the Lee-Yang-Parr gradient-corrected correlation potential (B3LYP) [24–27], and all calculations were performed without any symmetry constraints by using 6-31G** basis set. The electronic absorption spectra require calculation of the allowed excitations and oscillator strengths. The TDDFT has been used to investigate the absorption properties of clusters and molecules which has been proved to be an efficient approach [28, 29]. The iodine/iodide couple is used as regenerator in DSCs, implying that the solar cells work in solvent phase. Thus UV/Vis experimental data for triphenylamine-based dyes are reported in solvent. The polarizable continuum model (PCM) [30–34] is used for evaluating bulk solvent effects at all stages. The long-range-corrected (LC) functionals are good to reproduce the excitation energies for donor-bridge-acceptor systems which are more efficient in many cases [35]. The charge-transfer excitations in donor-bridge-acceptor dyes have been computed by using LC density functional method [36–38]. The range-separation technique is based on a more physical model of the exchange potential. We have computed the excitation energy of parent molecule by LC functional (LC-BLYP) which underestimate the absorption spectra (see supporting information). The Preat et al. described that PCM-TDBHandHLYP/6-311 + G** level of theory is efficient to deal with the charge transfer (CT) in TPA based systems [39]. Thus absorption and CT have been probed at PCM-TDBHandHLYP/6-311 + G** level of theory. The calculations have been carried out in methanol according to the experimental set up [17].

Results and discussion

Electronic structure

The distribution patterns of highest occupied molecular orbitals (HOMOs) and lowest unoccupied molecular orbitals (LUMOs) of investigated sensitizers at ground states (S_0) are shown in Fig. 2. Generally, HOMOs are delocalized on TPA unit while LUMOs are localized on anchoring group, conjugated chain and the benzene ring near the anchoring group. This revealed that these materials would be excellent sensitizers as comprehensible charge transfer has been observed from donor to acceptor side thus electron injection from TPA moiety to TiO_2 conduction band would be favorable.

In Table 1, HOMO energy (E_{HOMO}), LUMO energy (E_{LUMO}) and HOMO-LUMO energy gap (E_g) have been tabulated. The TC4 has HOMO and LUMO energies −5.30 eV and −2.56 eV, respectively have energy gap 2.74 eV. In TC4 there are two double bonds (four carbons) between TPA unit and anchoring group. By substituting the vinyl hydrogens with di-methyl enhanced the donor ability as well as two benzene rings as bridge and three double bonds (six carbons) between TPA moiety and anchoring group (**1**) leads to increasing the HOMO energy to −4.96 eV while lowering the LUMO energy to −2.86 eV compared to TC4 resulting in the energy gap 2.10 eV. Further increasing the double bonds up to four and two benzene rings as bridge (**2**) lower the LUMO energy to −2.93 eV leads to energy gap 2.02 eV. The **3** is similar to **1** except one additional benzene ring as bridge which leads to higher HOMO energy, lower LUMO energy and decreases the energy gap to 2.04 eV. Similarly, **4** is like **2** with the inclusion of one additional benzene ring as bridge which leads to higher HOMO energy (−4.91 eV), lower LUMO energy (−2.94 eV) and decreases the energy gap to 1.97 eV. Extending the bridge leads to higher HOMO and lowers the LUMO energies while decreasing the energy gap compared to TC4.

For good DSC sensitizers must have narrow band gap, LUMO lying just above the conduction band of TiO_2 and HOMO below the redox couple. The HOMO and LUMO energies of bare cluster $(TiO_2)_{38}$ are −7.23 and −4.1 eV, respectively, having HOMO–LUMO gap of 3.13 eV [40]. Usually an energy gap more than 0.2 eV between the LUMO of the dye and the conduction band of the TiO_2 is necessary for effective electron injection [41]. The LUMO energies of all the investigated dyes are above the conduction band of TiO_2. The HOMO of the redox couple (I^-/I_3^-) is −4.8 eV [42]. It can be found that HOMOs of the dyes are

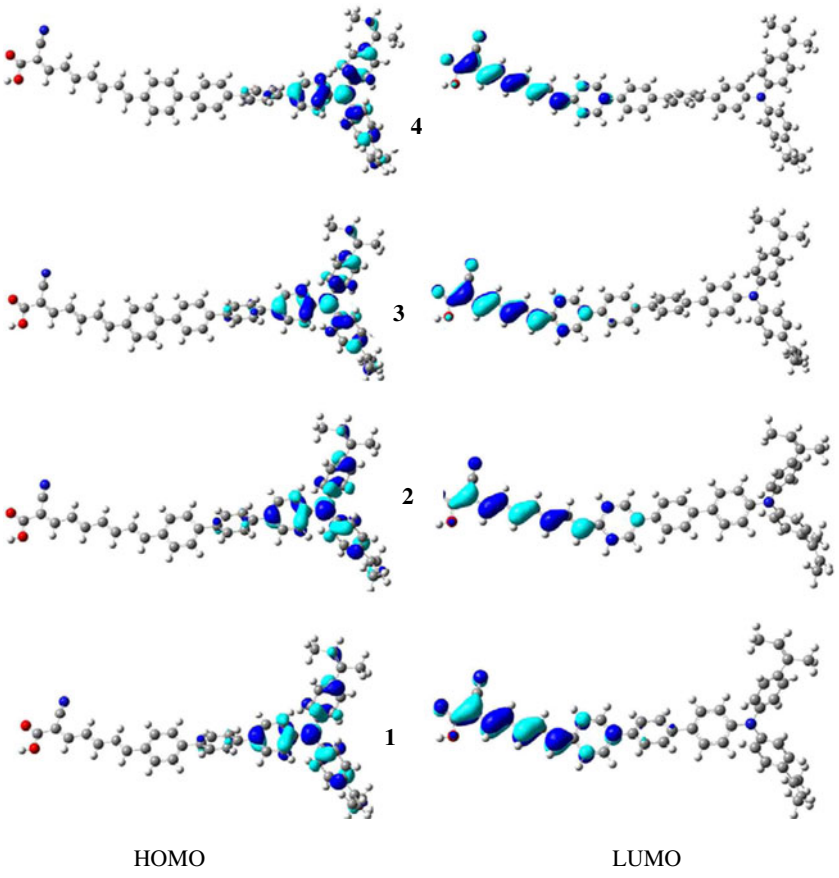

Fig. 2 The HOMO and LUMO distribution pattern of new designed sensitizers

Table 1 The HOMO energy (E_{HOMO}), LUMO energy (E_{LUMO}) and HOMO-LUMO energy gap (E_g) of TC4 and its derivatives in eV at B3LYP/6-31G** level of theory

Systems	E_{HOMO}	E_{LUMO}	E_g	Systems	E_{HOMO}	E_{LUMO}	E_g
1	−4.96	−2.86	2.10	3	−4.92	−2.88	2.04
2	−4.95	−2.93	2.02	4	−4.91	−2.94	1.97
TC4	−5.30	−2.56	2.74				

below the redox couple. The smaller HOMO-LUMO energy gaps of studied dyes compared to TC4 revealed that these dyes would be efficient for DSC. As designated by Fig. 2, the HOMO is delocalized over the pi-conjugated system with the highest electron density centered at the central TPA-nitrogen atom, and the LUMO is located in anchoring groups through the pi-bridge. It has been determined that the HOMO–LUMO excitation induced by light irradiation could move the electron distribution from the TPA-unit to the acceptor moiety and the photo-induced electron transfer from the dye to the TiO_2 electrode can occur efficiently by the HOMO–LUMO transition.

Electron injection

The description of the electron transfer from a dye to a semiconductor, the rate of the charge transfer process can be derived from the general classical Marcus theory [43–47],

$$k_{\text{inject.}} = |V_{RP}|\frac{2}{h}(\pi/\lambda k_B T)^{1/2}\exp\left[-\left(\Delta G^{\text{inject.}}+\lambda\right)^2/4\lambda k_B T\right]. \quad (1)$$

In Eq. (1), $k_{\text{inject.}}$ is the rate constant (in S^{-1}) of the electron injection from dye to TiO_2, k_{BT} is the Boltzmann thermal energy, h the Planck constant, - $\Delta G^{\text{inject.}}$ is the free energy of injection and λ is the reorganization energy of the system, $|V_{RP}|$ is the coupling constant between the reagent and the product potential curves. Equation (1) revealed that larger $|V_{RP}|$ leads to higher rate constant which would result better sensitizer. The value of $|V_{RP}|$ defines the adiabatic or non adiabatic character of the electron transfer, these two descriptions conveniently setting the limiting cases of a transition state formalism. The use of the generalized Mulliken-Hush formalism (GMH) allows evaluating |VRP| for a photoinduced charge transfer [41, 44]. Hsu et al. explained that |VRP| can be evaluated as [45]

$$|\text{VRP}| = \Delta E_{RP}/2. \quad (2)$$

The injection driving force can be formally expressed within Koopmans approximation as

$$\Delta E_{RP} = \left[E^{dye}_{LUMO} + 2E^{dye}_{HOMO}\right] - \left[E^{dye}_{LUMO} + E^{dye}_{HOMO} + E^{TiO2}_{CB}\right], \quad (3)$$

where E^{TiO2}_{CB} is the conduction band edge. Though it is often difficult to accurately determine E^{TiO2}_{CB} because it is highly sensitive to the conditions, e.g., the pH of the solution thus we have been using E^{TiO2}_{CB} =−4.0 eV [48], an experimental value corresponding to conditions where the semiconductor is in contact with aqueous redox electrolytes of fixed pH 7.0 [49, 50].

More quantitatively for a closed-shell system E^{dye}_{LUMO} corresponds to the reduction potential of the dye (E^{dye}_{RED}), whereas the HOMO energy is related to the potential of first oxidation (i.e., - $E^{dye}_{HOMO} = E^{dye}_{OX}$). As a result, Eq. (3) becomes,

$$\Delta E_{RP} = \left[E^{dye}_{HOMO} - E^{dye}_{OX}\right] = -\left[E^{dye}_{OX} + E^{TiO2}_{CB}\right]. \quad (4)$$

Equation (4) can be rewritten as

$$\Delta E_{RP} = E^{dye}_{0-0} - \left[2E^{dye}_{OX} + E^{dye}_{RED} + E^{TiO2}_{CB}\right]. \quad (5)$$

We propose to establish a reliable theoretical scheme to evaluate the dye's excited state oxidation potential, and quantify the electron injection onto a titanium dioxide (TiO_2) surface. The free energy change (in electron volts, eV) for the electron injection can be expressed as [49],

$$\Delta G^{\text{inject}} = E^{dye*}_{OX} - E^{TiO2}_{CB}, \quad (6)$$

where E^{dye*}_{OX} is the oxidation potential of the dye in the excited state, and E^{TiO2}_{CB} is the reduction potential of the semiconductor conduction band. Two models can be used for the evaluation of E^{dye*}_{OX} [43, 51, 52]. The first implies that the electron injection occurs from the unrelaxed excited state. For this reaction path, the excited state oxidation potential can be extracted from the redox potential of the ground state, E^{dye}_{OX} which has been calculated from the PCM-B3LYP-6-31G** approach using the restricted and unrestricted formalisms and the vertical transition energy corresponding to the photoinduced intramolecular CT (ICT),

$$E^{dye*}_{OX} = E^{dye}_{OX} - \lambda^{ICT}_{\max}, \quad (7)$$

where $\lambda^{ICT}_{\max}$ is the energy of the ICT. Note that this relation is only valid if the entropy change during the light absorption process can be neglected. For the second model, one assumes that electron injection occurs after relaxation. Given this condition, E^{dye*}_{OX} is expressed as [52]:

$$E^{dye*}_{OX} = E^{dye}_{OX} - E^{dye}_{0-0}, \quad (8)$$

where E^{dye}_{0-0} is the 0-0 transition energy between the ground state and the excited state. To estimate the 0-0 "absorption"

Table 2 The absorption spectra (λ_a)[a], $\Delta G^{inject.}$, oxidation potential, light harvesting efficiency and |VRP| of investigated dyes at TD-BHandHLYP/6-311+G**//B3LYP/6-31G** level of theory

System	λ_a	$\Delta G^{inject.}$	E_{OX}^{dye}	$E_{OX}^{dye^*}$	*cxx*	*f*	*LHE*	$\Delta G_r^{inject.}$	|VRP|
1	424	−1.95	4.97	2.05	2.92	2.5978	0.9975	1.17	0.975
2	456	−1.76	4.96	2.24	2.72	3.0755	0.9991	1.06	0.880
3	419	−2.00	4.96	2.00	2.96	2.7885	0.9984	1.20	1.00
4	453	−1.78	4.96	2.22	2.74	3.1578	0.9993	1.07	0.890
TC4	431	−1.66	5.22	2.34	2.88	1.5993	0.9748	1.00	0.830

ΔG_r^{inject} = relative electron injection ΔG^{inject}(dye)/ΔG^{inject}(TC4)

[a] Exp = The experimental absorption wavelengths of TC4 (425 nm) from ref. [17]

line, we need both the S_0 (singlet ground state) and the S_1 (first singlet excited state) equilibrium geometries, Q_{S0} and Q_{S1}, respectively.

Though electron injection from unrelaxed excited states has been observed in TiO_2 [53] and SnO_2 [54], the relative contribution of an ultrafast injection path is not clear, and most experimental groups assume that the electron injection dominantly occurs after relaxation [52]. Preat et al. concluded that the absolute difference between the relaxed and unrelaxed $\Delta G_{inject.}$ is constant for TPA derivatives, and is of the same order of magnitude as the E_{OX}^{dye} and E_{OX}^{dye*} mean average error (MAE) [55]. Here, ΔG^{inject} and E_{OX}^{dye*} have been evaluated using Eqs. (6) and (7).

The light harvesting efficiency (LHE) of the dye has to be as high as possible to maximize the photocurrent response. Here, LHE is expressed as [56]:

$$LHE = 1 - 10^{-A} = 1 - 10^{-f}, \quad (9)$$

where A (f) is the absorption (oscillator strength) of the dye associated to the λ_{max}^{ICT}. The oscillator strength is directly derived from the TDDFT calculations:

$$f = \frac{2}{3}\lambda_{max}^{ICT}\left|\overrightarrow{\mu}_{0-ICT}\right|^2, \quad (10)$$

where μ_{0-ICT} is the dipolar transition moment associated to the electronic excitation. In order to maximize f, both λ_{max}^{ICT} and μ_{0-ICT} must be large [57, 58].

We have presented the λ_a, ΔG^{inject}, E_{OX}^{dye}, E_{OX}^{dye*}, λ_{max}^{ICT}, LHE, RLHE, and ΔG_r^{inject} in Table 2. The computed absorption wavelengths have been tabulated in Table 2. The calculated absorption spectrum (λa) of TC4 (the parent system) is 431 nm in methanol which is in good agreement with the experimental data 425 nm [17]. Thus the absorption spectra of new designed dyes have been computed at TD-BHandHLYP/6-311 + G**//B3LYP/6-31G** level of theory by using PCM model in methanol. The **1** and **3** are 7 and 12 nm blue shifted while **2** and **4** are 25 and 22 nm red shifted, respectively compared to TC4. In parent molecule

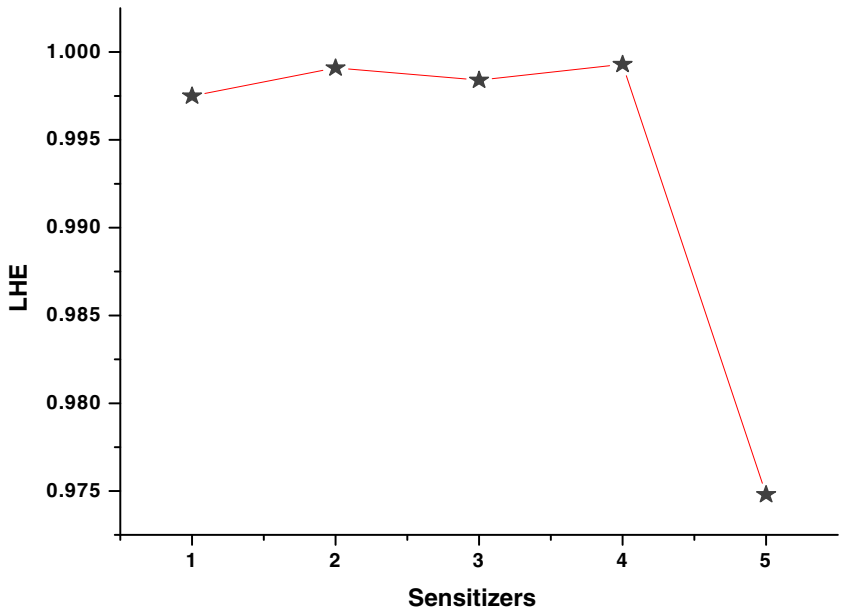

Fig. 3 The graph between light harvesting efficiency (LHE) along Y-axis and investigated sensitizers (**1**–**4**, TC4 (5)) in methanol along X-axis

(TC4), the ΔG^{inject} is −1.66 which augmented to −1.95 by increasing the two benzene rings between TPA and acceptor moieties and the double bonds up to three to further elongate the bridge (**1**). The ΔG^{inject} improved to −2.00 by increasing the three benzene rings between TPA and acceptor moieties (**3**). We have also observed that by increasing the double bonds to four with the two and three benzene rings between TPA and acceptor moieties in **2** and **4** diminish the ΔG^{inject} to −1.76 and −1.78, respectively. The ΔG^{inject} of new designed photosensitizers is superior to TC4. The ΔG_r^{inject} of **2** and **4** is 1.06 and 1.07 and **1** and **3** reach 1.17 and 1.20, respectively. In TC4, the electronic coupling constant |VRP| is 0.830 which improved to 0.975 by increasing the two benzene rings between TPA moiety and acceptor unit and the double bonds up to three to further elongate the bridge (**1**). The |VRP| reaches 1.00 by increasing the three benzene rings between TPA and acceptor moieties (**3**). It can be seen from Table 2 that by increasing the double bonds to four with two and three benzene rings between TPA moiety and acceptor unit in **2** and **4** reduces the |VRP| to 0.880 and 0.890, respectively. Generally, the |VRP| of new designed sensitizers (**1**–**4**) are higher than TC4. The trend of ΔG^{inject}, ΔG_r^{inject}, and |VRP| has been observed as **3**>**1**>**4**>**2**>TC4. The improved ΔG^{inject}, ΔG_r^{inject}, and |VRP| over TC4 is due to the reason that (1) di-methyl at two vinyl hydrogens at position 3 and 3' are greater electron donors which are favorable to promote the electron injection and electronic coupling constant. This can be verified by analyzing the distribution pattern of HOMOs and LUMOs of **1**–**4**. The comprehensive charge transfer has been observed from donor to acceptor moieties. (2) Enhanced bridge encourages the promotion of the electron injection and electronic coupling constant. The LHE of TC4 is 0.9748 which augmented to 0.9975 in **1**. The LHE further improved to 0.9984 by increasing the three benzene rings between TPA and acceptor moieties (**3**). Elongating the bridge (increasing the double bonds to four) enhanced the LHE to 0.9991 and 0.9993 in **2** and **4**, respectively. Figure 3 illustrated the light harvesting efficiency (LHE) on Y-axis of different investigated sensitizers. The LHE for **1**–**4** is the higher than TC4.

Undeniably, the TPA moiety shows a sizable steric hindrance and is expected to greatly favor the detention of the cationic charge from the semiconductor surface and efficiently obstruct the recombination [16]. We have explained the recombination barricade on the basis of distortion and coplanarity. The coplanarity between the benzene near anchoring group having LUMO and the last benzene attached to TPA unit is broken in **1**–**4** compared to TC4, i.e., 34–35° out-of-plane distortion, thus the positive charge may not be directly in drop line to the TiO_2 surface, consequently hampering the recombination reaction.

Conclusions

In the framework of our present quantum chemical investigation, we can draw the following conclusions:

1. The HOMOs are delocalized over the pi-conjugated systems with the highest electron density centered at the central TPA-nitrogen atom, and the LUMOs are located at the anchoring groups through the pi-bridge. Generally, HOMOs are delocalized on donor moieties while LUMOs are localized toward anchoring groups.
2. The comprehensible charge transfer has been observed from donor to acceptor side.
3. The elongation of the bridge leads to higher HOMO energies, lower LUMO energies and decreases the energy gap.
4. The LUMO energies are above the conduction band of TiO_2, and HOMO energies below the redox couple.
5. The calculated absorption spectrum of TC4 is 431 nm in methanol which is in good agreement with the experimental data 425 nm. The **1** and **3** are 7 and 12 nm blue shifted while **2** and **4** are 25 and 22 nm red shifted, respectively compared to TC4.
6. The ΔG^{inject} of new designed photosensitizers is superior to TC4. The |VRP| of new designed sensitizers (**1**–**4**) is also higher than TC4. The trend of ΔG^{inject}, ΔG_r^{inject}, and |VRP| has been observed as **3**>**1**>**4**>**2**>TC4.
7. The enhanced bridge encourages the promotion of the electron injection electronic, coupling constant and light harvesting efficiency.
8. The coplanarity between the benzene near anchoring group having LUMO and the last benzene attached to TPA unit is broken in **1**–**4** compared to TC4, i.e., 34–35° out-of-plane distortion, thus the positive charge may not be directly in drop line to the TiO_2 surface, consequently hampering the recombination reaction.

Acknowledgements We are thankful to the King Khalid University for the support and facilities provided to carry out this research work.

References

1. Regan BO, Gratzel M (1991) A low-cost, high-efficiency solar cell based on dye- sensitized colloidal TiO2 films. Nature 353:737–740
2. Nazeeruddin MK, De Angelis F, Fantacci S, Selloni A, Viscardi G, Liska P, Ito S, Takeru B, Grätzel M (2005) Combined experimental and DFT-TDDFT computational study of photoelectrochemical cell ruthenium sensitizers. J Am Chem Soc 127:16835–16847
3. Zhang QF, Dandeneau CS, Zhou XY, Cao GZ (2009) ZnO nanostructures for dye-sensitized solar cells. Adv Mater 21:4087–4108
4. Li G, Jiang KJ, Li YF, Li SL, Yang LM (2008) Efficient structural modification of triphenylamine-based organic dyes for dye-sensitized solar cells. J Phys Chem C 112:11591–11599
5. Wong BM, Codaro JG (2008) Coumarin dyes for dye-sensitized solar cells: a long-range-corrected density functional study. J Chem Phys 129:214703–214710

6. Horiuchi T, Miura H, Sumioka K, Uchida S (2004) High efficiency of dye-sensitized solar cells based on metal-free indoline dyes. J Am Chem Soc 126:12218–12219
7. Stathatos E, Lianos P, Laschewsky A, Ouari O, Van Cleuvenbergen P (2001) Synthesis of a hemicyanine dye bearing two carboxylic groups and its use as a photosensitizer in dye-Sensitized photoelectrochemical cells. Chem Mater 13:3888–3892
8. Baik C, Kim D, Kang MS, Song K, Sang OK, Ko J (2009) Synthesis and photovoltaic properties of novel organic sensitizers containing indolo[1,2-f]phenanthridine for solar cell. Tetrahedron 65:5302–5307
9. Ferrere S, Zaban A, Gregg B (1997) Dye sensitization of nanocrystalline tin oxide by perylene derivatives. J Phys Chem B 101:4490–4493
10. Nilsing M, Persson P, Lunell S, Ojamäe L (2007) Dye-sensitization of the TiO2 rutile (110) surface by perylene dyes: Quantum-chemical periodic B3LYP computations. J Phys Chem C 111:12116
11. Robertson N (2006) Optimizing dyes for dye-sensitized solar cells. Angew Chem Int Ed 45:2338–2345
12. Liu D, Fessenden RW, Hug GL, Kamat PV (1997) Dye capped semiconductor nanoclusters. Role of back electron transfer in the photosensitization of SnO_2 nanocrystallites with cresyl violet aggregates. J Phys Chem B 101:2583–2590
13. Burfeindt B, Hannappel T, Storck W, Willig F (1996) Measurement of temperature-independent femtosecond interfacial electron transfer from an anchored molecular electron donor to a semiconductor as acceptor. J Phys Chem 100:16463–16465
14. Sayama K, Tsukagochi S, Hara K, Ohga Y, Shinpou A, Abe Y, Suga S, Arakawa H (2002) Photoelectrochemical properties of J aggregates of benzothiazole merocyanine dyes on a nanostructured TiO_2 film. J Phys Chem B 106:1363–1371
15. Hagfeldt A, Gratzel M (2000) Molecular photovoltaics. Acc Chem Res 33:269–277
16. Ning Z, Zhang Q, Wu W, Pei H, Liu B, Tian H (2008) Starburst triarylamine based dyes for efficient dye-sensitized solar cells. J Org Chem 73:3791–3797
17. Xu W, Peng B, Chen J, Liang M, Cai F (2008) New triphenylamine-based dyes for dye-sensitized solar cells. J Phys Chem C 112:874–880
18. Irfan A, Al-Sehemi AG, Asiri AM (2012) Donor-enhanced bridge effect on the electronic properties of triphenylamine based dyes: density functional theory investigations. J Mol Model. doi:10.1007/s00894-012-1372-9
19. Irfan A, Cui R, Zhang J, Hao L (2009) Push–pull effect on the charge transfer, and tuning of emitting color for disubstituted derivatives of mer-Alq3. Chem Phys 364:39–45
20. Preat J, Michaux C, Jacquemin D, Perpete EA (2009) Enhanced efficiency of organic dye-sensitized solar cells: triphenylamine derivatives. J Phys Chem C 113:16821–16833
21. Irfan A, Aftab H, Al-Sehemi AG (2012) Push–pull effect on the geometries, electronic and optical properties of thiophene based dye-sensitized solar cell materials. J Saudi Chem Soc. doi:10.1016/j.jscs.2011.11.013
22. Al-Sehemi AG, Irfan A, Asiri AM, Ammar YA (2012) Synthesis, characterization and DFT study of methoxybenzylidene containing chromophores for DSSC materials. Spectrochim Acta A 91:239–243
23. Frisch MJ et al (2009) Gaussian 09, Revision A.1. Gaussian Inc, Wallingford, CT
24. Becke AD (1993) Density–functional thermochemistry. III. The role of exact exchange. J Chem Phys 98:5648–5652
25. Miehlich B, Savin A, Stoll H, Preuss H (1989) Results obtained with the correlation energy density functionals of Becke and Lee, Yang and Parr. Chem Phys Lett 157:200–206
26. Lee C, Yang W, Parr RG (1988) Development of the Colle-Salvetti correlation-energy formula into a functional of the electron density. Phys Rev B 37:785–789
27. Sun J, Song J, Zhao Y, Liang WZ (2007) Real-time propagation of the reduced one-electron density matrix in atom-centered Gaussian orbitals: application to absorption spectra of silicon clusters. J Chem Phys 127:234107–234113
28. Zhang CR, Liang WZ, Chen HS, Chen YH, Wei ZQ, Wu YZ (2008) Theoretical studies on the geometrical and electronic structures of N-methyle-3,4-fulleropyrrolidine. J Mol Struct THEOCHEM 862:98–104
29. Matthews D, Infelta P, Grätzel M (1996) Sol Energy Mater Sol Cells 44:119–155
30. Cossi M, Barone V (2001) Time-dependent density functional theory for molecules in liquid solutions. J Chem Phys 115:4708–4717
31. Amovilli C, Barone V, Cammi R, Cancès E, Cossi M, Mennucci B, Pomelli CS, Tomasi J (1998) Recent advances in the description of solvent effects with the polarizable continuum model. Adv Quant Chem 32:227–261
32. Tomasi J, Mennucci B, Cammi R (2005) Quantum mechanical continuum solvation models. Chem Rev 105:2999–3094
33. Barone V, Cossi M (1998) Quantum calculation of molecular energies and energy gradients in solution by a conductor solvent model. J Phys Chem A 102:1995–2001
34. Cossi M, Rega N, Scalmani G, Barone V (2003) Energies, structures, and electronic properties of molecules in solution with the C-PCM solvation model. J Comput Chem 24:669–681
35. Peach MJG, Benfield P, Helgaker T, Tozer DJ (2008) Excitation energies in density functional theory: an evaluation and a diagnostic test. J Chem Phys 128:044118
36. Stein T, Kronik L, Baer R (2009) Prediction of charge-transfer excitations in coumarin-based dyes using a range-separated functional tuned from first principles. J Chem Phys 131:244119–244123
37. Wong BM, Piacenza M, Sala FD (2009) Absorption and fluorescence properties of oligothiophene biomarkers from long-range-corrected time-dependent density functional theory. Phys Chem Chem Phys 11:4498–4508
38. Wong BM, Cordaro JG (2008) Coumarin dyes for dye-sensitized solar cells: a long-range-corrected density functional study. J Chem Phys 129:214703–214710
39. Preat J, Jacquemin D, Perpete E (2010) Design of new triphenylamine-sensitized solar cells: a theoretical approach. Environ Sci Technol 44:5666–5671
40. Balanay MP, Kim DH (2008) DFT/TD-DFT molecular design of porphyrin analogues for use in dye-sensitized solar cells. Phys Chem Chem Phys 10:5121–5127
41. De Angelis F, Fantacci S, Selloni A (2008) Alignment of the dye's molecular levels with the TiO_2 band edges in dye-sensitized solar cells: a DFT–TDDFT study. Nanotechnology 19:424002–424008
42. Ito S, Zakeeruddin SM, Humphry-Baker R, Liska P, Charvet R, Comte P, MdK N, Pechy P, Takata M, Miura H, Uchida S, Gratzel M (2006) High-efficiency organic-dye-sensitized solar cells controlled by nanocrystalline-TiO_2 electrode thickness. Adv Mater 18:1202–1205
43. Matthews D, Infelta P, Grätzel M (1996) Calculation of the photocurrent-potential characteristic for regenerative, sensitized semiconductor. Sol Energ Mater Sol Cells 44:119–155
44. Pourtois G, Beljonne J, Ratner MA, Bredas JL (2002) Photoinduced electron-transfer processes along molecular wires based on phenylenevinylene oligomers: a quantum-chemical insight. J Am Chem Soc 124:4436–4447
45. Hsu C (2009) The electronic couplings in electron transfer and excitation energy transfer. Acc Chem Res 42:509–518
46. Marcus RA (1993) Electron transfer reactions in chemistry. Theory and experiment. Rev Mod Phys 65:599–610
47. Higendorff M, Sundstrom V (1998) Dynamics of electron injection and recombination of dye-sensitized TiO_2 particles. J Phys Chem B 102:10505–10514

48. Asbury JB, Wang YQ, Hao E, Ghosh H, Lian T (2001) Evidences of hot excited state electron injection from sensitizer molecules to TiO2 nanocrystalline thin films. Res Chem Intermed 27:393–406
49. Katoh R, Furube A, Yoshihara T, Hara K, Fujihashi G, Takano S, Murata S, Arakawa H, Tachiya M (2004) Efficiencies of electron injection from excited N3 dye into nanocrystalline semiconductor (ZrO_2, TiO_2, ZnO, Nb_2O_5, SnO_2, In_2O_3) films. J Phys Chem B 108:4818–4822
50. Hagfeldt A, Grätzel M (1995) Light-induced redox reactions in nanocrystalline systems. Chem Rev 95:49–68
51. Barbara PF, Meyer TJ, Ratner MA (1996) Contemporary issues in electron transfer research. J Phys Chem 100:13148–13168
52. De Angelis F, Fantacci S, Selloni A (2008) Alignment of the dye's molecular levels with the TiO_2 band edges in dye-sensitized solar cells: a DFT–TDDFT study. Nanotechnology 19:424002–424008
53. Benkö G, Kallioien J, Korppi-Tommola JEI, Yartsev AP, Sundström V (2002) Photoinduced ultrafast dye-to-semiconductor electron injection from nonthermalized and thermalized donor states. J Am Chem Soc 124:489–493
54. Iwa S, Hara K, Murata S, Katoh R, Sugihara H, Arakawa H (2000) Ultrafast interfacial charge separation processes from the singlet and triplet MLCT states of Ru(bpy)2(dcbpy) adsorbed on nanocrystalline SnO2 under negative applied bias. J Chem Phys 113:3366–3373
55. Preat J, Michaux C, Jacquemin D, Perpète EA (2009) Enhanced efficiency of organic dye-sensitized solar cells: triphenylamine derivatives. J Phys Chem C 113:16821–16833
56. Nalwa HS (2001) Handbook of advanced electronic and photonic materials and devices. Academic, San Diego
57. Cassida M (1995) Recent advances in density functional methods: time dependent density functional response theory for molecules. Chong, Singapore
58. Harris DC, Bertolucci MD (1998) Symmetry and spectroscopy. Dover, New York